Bending-Sensitive Optical Waveguide Sensor With Carbon-Fiber Layer for Monitoring Grip Strength

Wuxiang Zhang, *Member, IEEE*, Hanze Jia, Linhang Ju, *Student Member, IEEE*, Yanjun Shi, Xilun Ding, and Yanggang Feng, *Member, IEEE*

***Abstract*— With the gradual popularity of wearable devices, the demand for high-performance flexible wearable sensors is also increasing. Flexible sensors based on the optical principle have advantages *e.g.* anti-electromagnetic interference, antiperspirant, inherent electrical safety, and the potential for biocompatibility. In this study, an optical waveguide sensor integrating a carbon fiber layer, fully constraining stretching deformation, partly constraining pressing deformation, and allowing bending deformation, was proposed. The sensitivity of the proposed sensor is three times higher than that of the sensor without a carbon fiber layer, and good repeatability is maintained. We also attached the proposed sensor to the upper limb to monitor grip force, and the sensor signal showed a good correlation with grip force (the R-squared of the quadratic polynomial fitting was 0.9827) and showed a linear relationship when the grip force was greater than 10 N (the R-squared of the linear fitting was 0.9523). The proposed sensor has the potential for applications in recognizing the intention of human movement to help the amputees control the prostheses.**

***Index Terms*— Optical waveguide, soft sensor, wearable devices, grip strength.**

I. Introduction

MILLIONS of people worldwide have their limbs amputated for traumatic reasons [1]. To allow amputees to regain normal limb function [2], robotic prostheses were developed. Meanwhile, research on soft sensors is gaining momentum, with greater potential for human-machine interaction safety, adaptability to disturbances, and flexibility to changes in task settings than rigid mechanisms [3]. Wearable sensors are widely used for health detection [4], [5], [6] and motion analysis [5] due to their good flexibility, varied structural forms, and arbitrary arrangement according to the actual situation [6].

Current flexible wearable sensors mostly use resistive [7], [8], capacitive [9], [10], [11], or optical [12], [13], [14], [15], [16], [17] detection principles. In contrast to resistive and capacitive principles, optical principles offer unique advantages in terms of anti-electromagnetic interference, antiperspirant, inherent electrical safety, and the potential for biocompatibility, which have good implications for advancing human- machine interaction [18]. The principles of light spectrum using fiber Bragg grating [12], [13], [14], [15] or light intensity using optical fiber [16], [17] to flexible sensors to detect deformations has been shown to be feasible. However, bulky external devices, such as laser light sources, and fiber grating demodulators, make the whole sensor bulky and not easy to wear. The optical fiber used to make the sensor also reduces the wearing comfort. To deal with these challenges, flexible optical waveguide sensors based on measuring the loss of light intensity were developed. The flexible optical waveguide sensor has two parts, *i.e.*, the core and the cladding. Due to their different refractive indices, light can propagate in the core through the reflection of the cladding, thus giving the optical waveguide the properties of an optical fiber [19]. Simultaneous detection of bending, stretching, and pressing deformations with a single flexible optical waveguide sensor has been achieved [20]. Soft prosthetic hands have also obtained excellent sensing capabilities by integrating optical waveguide sensors [21]. A stretchable distributed fiber-optic sensor was developed that can distinguish and measure the locations, magnitudes, and modes (bend, stretch, or press) of mechanical deformation [22].

The sensor using the optical waveguide principle has the following features. Bending, stretching, and pressing deformations will lead to the optical waveguide changes in light intensity, and these changes are not independent of each other. The information about the three-dimension changes in the

Manuscript received 27 December 2022; revised 20 February 2023 and 23 March 2023; accepted 27 March 2023. Date of publication 29 March 2023; date of current version 5 April 2023. This work was supported in part by the National Natural Science Foundation of China (NSFC) under Grant T2121003 and Grant 91848104, and in part by the Young Talent Program of Beihang University under Grant KG16168401. *(Corresponding author: Yanggang Feng.)*

This work involved human subjects or animals in its research. Approval of all ethical and experimental procedures and protocols was granted by the Local Ethics Committee of Beihang University under Application No. BM20220209, and performed in line with the Declaration of Helsinki.

Wuxiang Zhang and Xilun Ding are with the School of Mechanical Engineering and Automation and the Beijing Advanced Innovation Centre for Biomedical Engineering, Beihang University, Beijing 100191, China.

Hanze Jia, Linhang Ju, Yanjun Shi, and Yanggang Feng are with the School of Mechanical Engineering and Automation, Beihang University, Beijing 100191, China (e-mail: yanggangfeng@buaa.edu.cn).

Digital Object Identifier 10.1109/TNSRE.2023.3263227

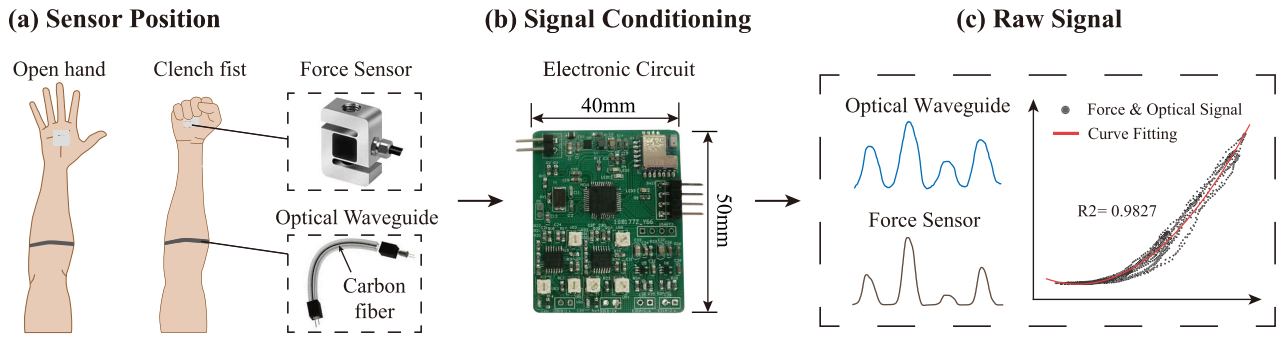

Fig. 1. Overview of this study. (a) Sensor position of this study. (b) Signal conditioning circuit. (c) Force sensor vs. optical waveguide raw signal comparison.

signal can make it more difficult to analyze the cause of the change in light intensity. Consequently, three-dimension changes increase the difficulty of finding the exact mapping relationship between deformation and optical signal. For instance, the deformation of the optical waveguide sensor is allowed in three dimensions, which increases the sensitivity of the sensor, and, consequently, makes soft hand prosthesis obtain sensing capabilities [21]. However, for muscle activity monitoring, muscle deformation will lead to multiple changes in the optical waveguide sensor, increasing the difficulty of finding the exact mapping relationship between deformation and optical signal.

In this study, an optical waveguide sensor integrating a carbon fiber layer, fully constraining stretching deformation, partly constraining pressing deformation, and allowing bending deformation, was proposed. The nature of carbon fiber as flexible as silk threads, a density of 1.4 g/cm^3, a diameter of 7 μ m, and a tensile coefficient of no more than 1.6% [23], showed anti-stretching, and anti-pressing properties. Based on these properties, we constrained the stretching deformation of the optical waveguide by embedding a carbon fiber layer between the core and the cladding, thus constraining the effect of stretching on the change in light intensity. Also, embedding the carbon fiber layer into the optical waveguide sensor, partly constrained pressing deformation. Bending deformation was allowed in the proposed sensor. We also attached the proposed sensor to a human upper limb to detect the change in grip strength when clenching the fist. For comparison, a force sensor was placed in the hand to measure the grip strength(shown in Fig. 1a). Fig. 1b showed the signal conditioning circuit which can convert the change in light intensity that occurs when the optical waveguide is bent into a voltage change that can be measured. We fitted the raw signals of the force sensor and the optical waveguide sensor with a polynomial. As shown in Fig. 1c, a strong correlation between the signals of the force sensor and the optical waveguide sensor can be obtained.

II. Sensor Design

In this section, we introduce the working principle of the optical waveguide sensor, the method of fabricating the optical waveguide, and the components of the sensor.

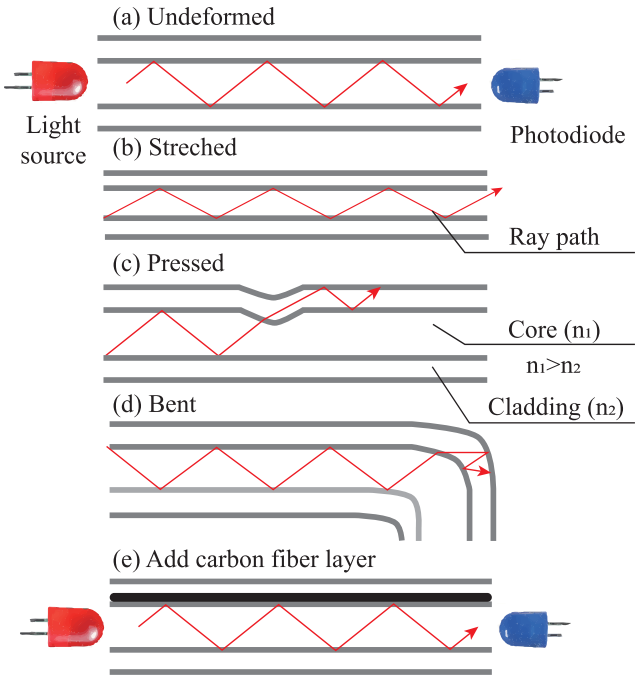

Fig. 2. The principle of total internal reflection and the proposed sensor design. Ray diagram of the optical waveguide when it is (a) undeformed, (b) stretched, (c) pressed, (d) bent. (e) The proposed sensor design.

A. Working Principle of Waveguide

The optical waveguide works on the principle of total internal reflection, illustrated in Fig. 2. The optical waveguide is made of two flexible light-transmitting materials with different refractive indices: the core (refractive index of n_1) and the cladding (refractive index of n_2, $n_1 > n_2$). When light enters from the medium with a higher refractive index (n_1) to the medium with a lower refractive index (n_2), if the angle of incidence θ_1 is greater than a certain critical angle θ_c (eq.1), the refracted light will disappear, and all the incident light will be reflected without entering the medium with lower refractive index.

$$\theta_c = \arcsin\left(\frac{n_2}{n_1}\right) \tag{1}$$

As shown in Fig. 2a, in the undeformed state, the light source (LED) at one end of the optical waveguide emits infrared

TABLE I
CORE AND CLADDING MATERIAL PROPERTIES

	Clear Flex 30 (Core)	Dragon Skin 20 (Cladding)
Refractive	1.47	1.41
Color	Clear	Translucent
Shore A hardness	30	20
Elongation at break	675%	620%
Tensile strength	725psi	550psi
Linear shrinkage	<0.1%	<0.1%

light that passes through the core with very little light loss, and the photodiode senses the unlost light at the other end. When the optical waveguide is in a stretched, bent, or pressed state, some light passing through the core will be lost(shown in Fig. 2,b, c, and d). Based on this principle, the magnitude of the deformation can be reflected by detecting the change of light intensity in the optical waveguide. Obviously, these three deformations interact with each other, which increases the difficulty of finding the exact mapping relationship between deformation and optical signal. So, we embedded a carbon fiber layer between the core and the cladding of the optical waveguide in order to fully constrain stretching deformation, partly constrain pressing deformation, but allow bending deformation. Consequently, the change of light intensity of the optical waveguide will mainly come from the bending deformation, which is significant for building the relationship between bending and sensor signal. The reason for choosing carbon fiber is its 1.4 g/cm^3 density, 7 μ m diameter, and tensile coefficient of no more than 1.6%.

We used an LED (TSHA4400, Vishay Semconductors; peak wavelength: 875nm) as the light source and a photodiode (SFH229, OSRAM Licht AG; spectral range: 380nm to 1100nm) as the light detector. The optical waveguide sensor is made of two elastomers, a polyurethane elastomer core with a higher refractive index (Clear Flex 30, $n_{core} = 1.47$, Smooth-on Inc.) and a silicon elastomer cladding with a lower refractive index(Dragon Skin 20, $n_{cladding} = 1.41$, Smooth-on Inc.). And the two material properties are given in Table I. The reasons for choosing these two materials are as follows:

(1) The refractive index of the core material is higher than that of the cladding material, and the larger refractive index difference can increase the sensitivity of the optical waveguide to light intensity loss.

(2) The core has high transmittance to the shortwave infrared.

(3) The core and cladding materials need to have similar mechanical properties to avoid unwanted effects of mechanical mismatch.

In addition, the very low stiffness gives the optical waveguide a soft texture, and the excellent tensile strength and linear shrinkage make the optical waveguide less susceptible to damage, which has good potential for the sensor to be used in soft robots. We also designed our own signal conditioning circuitry to collect light intensity data at a sampling rate of 100 Hz (shown in Fig. 1b). And we used a battery to power the signal conditioning circuit, which measures 30 mm in length, 20 mm in width, and 5 mm in thickness, with a capacity of 50 mAh and a rated voltage of 8 V.

B. Waveguide Bending Loss

The embedding of the carbon fiber layer limits the stretching and pressing deformation of the optical waveguide, so we ignore the light loss caused by these two factors and only consider the light loss caused by the bending deformation. Calculating the light loss due to bending deformation is very complicated, but it is good that there has been research [24] to prove that there is a clear mathematical relationship between light loss α and bending radius R:

$$\begin{cases} \alpha = \frac{1}{8}\sqrt{\frac{2\pi}{3}}\frac{1}{A_{eff}}\frac{1}{\beta}F\left[\frac{2}{3}R\frac{\left(\beta^2-\beta_c^2\right)^{3/2}}{\beta^2}\right] \\ F(x) = x^{-\frac{1}{2}}e^{-x} \\ \beta = \frac{2\pi n_1}{\lambda} \\ \beta_c = \frac{2\pi n_2}{\lambda} \end{cases} \tag{2}$$

A_{eff} is the effective area which can be calculated by using the following equation:

$$A_{eff} = \frac{\left[\int I(r)\, r dr\right]^2}{\left[\int I^2(r)\, dr\right]^2} \tag{3}$$

where $I(r) = |E_t|^2$ is the transverse electric field intensity distribution in the optical waveguide cross-section. It is obvious that after the materials and dimensions of the core and cladding of the optical waveguide are determined, only one variable, R, is in the formula. Therefore, it can be assumed that the optical waveguide sensor with carbon fiber can accurately monitor the change of bending radius by light loss.

C. Fabrication of Waveguide

We fabricated the optical waveguide through replica molding and laminating polyurethane and silicone Elastomers (shown in Fig. 3a):

(1) Two acrylic molds are machined using CNC machining methods, which are used to fabricate the cladding and core.

(2) Inject the core(Clear Flex 30) and cladding(Dragon Skin 20) into the mold made in the first step with a syringe, and wait for the elastomer to solidify for 24 hours.

(3) Place the core into the cladding and place the carbon fiber(T300-1K; elongation: 1.5%) on top of the core.

(4) Use a syringe to inject Dragon Skin 20 into the cladding space. After waiting for 24 hours for the elastomer to solidify, an optical waveguide with a carbon fiber layer can be obtained.

There are two reasons for using acrylic molds:

(1) Compared to 3D-printed molds, acrylic molds have a smooth surface, contributing to light propagation in polyurethane elastomers.

(2) 3D-printed molds can leave some residual trace elements on the surface after fabrication. In our experiments, we found that the residual elements on the surface of 3D-printed molds would inhibit the curing of polyurethane elastomers and make

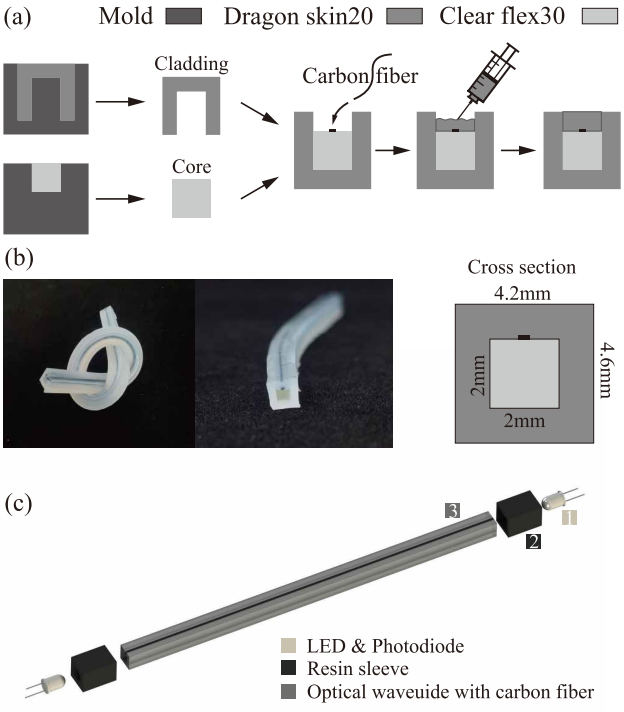

Fig. 3. Fabrication and structure of the optical waveguide sensor. (a) Fabrication process of the optical waveguide. (b) Photo and cross-sectional view of the optical waveguide. (c) Exploded view of the optical waveguide sensor with carbon fiber.

it more difficult to be de-molded, and this phenomenon cannot be solved by using release agents.

It is important to note that when making the core or cladding, it is necessary to mix all components thoroughly and evacuate the air bubbles inside under a vacuum, which is the key to ensuring the light-guiding performance of the light waveguide. As shown in Fig. 3b, the cross-section of the core (Clear Flex 30) is 2mm × 2mm and the cladding (Dragon Skin 20) is 4.2mm × 4.6mm, which makes the whole optical waveguide very small and can reduce the foreign body feeling when people wear it. In addition, the almost inextensible carbon fiber constrains the stretching deformation of the optical waveguide, which makes the sensor more sensitive to changes in curvature. The photos in Fig. 3b show an actual optical waveguide with carbon fiber. The first one is a knotted optical waveguide, which fully demonstrates its flexibility. The second photo shows a close-up of a normally placed optical waveguide with a cross-section.

The optical waveguide sensor with a carbon fiber layer consists of three parts (shown in Fig. 3c): LED & photodiode, an optical waveguide with a carbon fiber layer, and a resin sleeve. The light source (LED) and the light detector (photodiode), which senses the change of light intensity, are at the two ends of the sensor, and the optical waveguide with a carbon fiber layer is in the middle. These two are connected by a resin sleeve made by 3D printing. This design allows for more flexibility in the sensor assembly. It is not necessary to replace the entire sensor in case of partial damage. Only the damaged part needs to be replaced.

III. Experimental Evaluation

In this section, we introduce the comparison of the response of the proposed sensor and the optical waveguide sensor without a carbon fiber layer to three kinds of deformations (bending, pressure, and stretching).

In general, optical waveguides are subjected to deformations such as bending, pressing, and stretching, but because of the non-stretchable carbon fiber in the optical waveguide, the stretching deformation of the sensor is fully constrained, and the pressure of the sensor is partly constrained. This allows us to consider only the effect of bending and pressure on the sensor signal. Therefore, we tested the performance of the optical waveguide sensor in different bending and pressing states and compared the two optical waveguide sensors with and without a carbon fiber layer. And the response of the optical waveguide sensor without a carbon fiber layer during being stretched was also tested. In addition, to make the comparison of two optical waveguide sensors more intuitive, The voltage of the signal modulation circuit when the optical waveguide sensor has no deformation is defined as V_0. And the voltage of the signal modulation circuit when the optical waveguide sensor has deformation is V, so the signal loss ratio is defined as [25]

$$r = \frac{V}{V_0} \tag{4}$$

The voltage of the signal modulation circuit increases as the light intensity decreases. So, based on this definition, we can then build a relationship between r and deformation: the greater the curvature of the optical waveguide, the greater r, and the greater the force, the greater r. This makes it possible to compare the sensitivity of the two optical waveguide sensors to bending and pressure.

A. Response to Bending

Two optical waveguide sensors were used for comparison, one fabricated with a carbon fiber layer and the other without a carbon fiber layer, as shown in Fig. 4a. To reduce the influence of other factors on experimental results in the bending experiments, two optical waveguide sensors were fabricated with the same mold and at the same length (80mm). Fig. 4b depicted a 3D-printed bending experimental platform. The platform was designed with nine grooves of different curvatures, which were evenly distributed from 0 to 40 m^{-1}. The optical waveguide sensor was placed firmly in the groove of the bending experimental platform and maintained the same curvature as the groove. A uniform curvature of the grooves led to a uniform bending of the optical waveguide sensor.

In the bending test, the light intensity loss of the two optical waveguides was tested in the range from 0 to 40 m^{-1} curvature, and a test was repeated 10 times. Fig. 5a depicted the results of the test, and an optical waveguide with a carbon fiber layer has a more sensitive optical intensity loss than a sensor without a carbon fiber layer. The light intensity loss ratio of the optical waveguide with a carbon fiber layer is about three times higher than a sensor without a carbon fiber layer. In addition, both optical waveguides indicated an almost

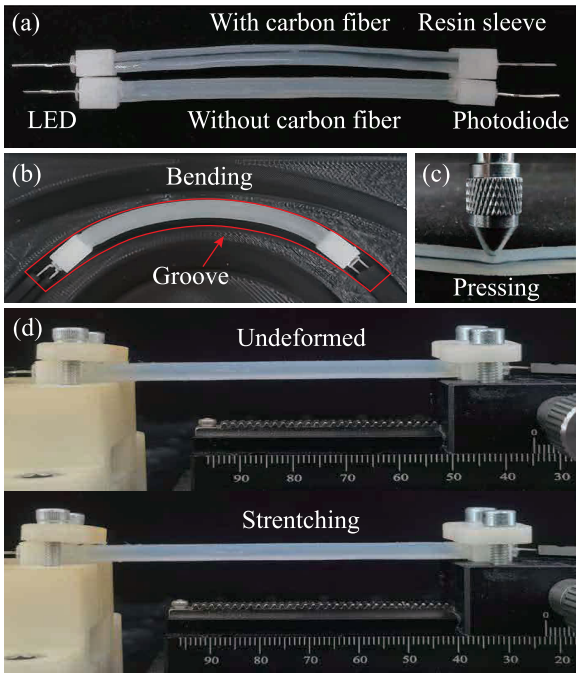

Fig. 4. Optical waveguide sensor characterization test method. (a) Two optical waveguide sensors with and without a carbon fiber layer. (b) Bending test platform. (c) Pressing test platform. (d) Stretching test platform.

linear relationship with curvature, which has good implications for building the mapping relationship between curvature and sensor signals.

B. Response to Pressing

The characteristics of two optical waveguide sensors under pressure were also tested. A press (HLD, FUMA Ltd.) was used to apply pressure to the optical waveguide sensors, and the press was equipped with an electronic push-pull gauge (SH-200, HANDPI Ltd.) with a division of 0.01 N, which ensured the accuracy of recording the force applied to the optical waveguide sensors. The point type used for the indenter of the press (Fig. 4c) has a contact area of 4 mm^2 with the optical waveguide. The tiny contact area can generate a large pressure. The pressure was applied from zero, and the light loss of the optical waveguide was recorded for every 0.1N increase. As shown in Fig. 5b, the maximum pressure applied in the pressure test reached 1 N (250,KPa). Clearly, the sensitivity of the optical waveguide sensor with a carbon fiber layer to pressure becomes lower than the optical waveguide without a carbon fiber layer due to the stretch resistance of carbon fiber and shows better linearity from 0-0.3 N or even throughout the pressurization process. This result fully demonstrates that the carbon fiber layer has some ability to constrain pressure deformation.

C. Response to Stretching

Fig. 4d shows the tensile test platform, which is the same as the one used in the bending experiments. The two photos in the Fig. 4d show the undeformed and stretched optical waveguide sensor without a carbon fiber layer. In the previous stretching tests [18], [22], a pre-stretch with an elongation greater than 10% was applied, which made us curious about the response of the optical waveguide sensor when the elongation was within 10%. So we tested the signal variation of the optical waveguide sensor without a carbon fiber layer at the elongation between 0 and 10%, and the tests were repeated 10 times. The optical waveguide is stretched when the linear guide rail is moved backward, and light loss of the optical waveguide was recorded for every 1% increase in elongation. Fig. 5c shows the results of the test, and it can be seen that the optical waveguide sensor without a carbon fiber layer did not show good repeatability when the elongation was less than 10%, and even a reduction in light intensity loss ratio occurred at the elongation of 1%. The reason for this phenomenon could be the interaction of three types of deformation(bending, pressing, and stretching) in the small deformation of the optical waveguide sensor. So, if you want to use a normal optical waveguide sensor without a carbon fiber layer to monitor bending deformation stably, you have to apply a pre-stretch. In contrast, the optical waveguide sensor with a carbon fiber layer cannot be stretched because it is embedded with anti-stretch carbon fiber, which avoids the slight stretching effect of the proposed sensor when monitoring bending deformation.

Silicone elastomers and polyurethane elastomers are common materials used in many soft robots, and these materials are identical to this optical waveguide [26], [27]. This proves that the optical waveguide is easy to combine with flexible devices. And after being embedded with a carbon fiber layer, the sensitivity of the optical waveguide to bending has been improved. To further test the performance of this optical waveguide sensor, we attached it to the upper limb to monitor grip strength.

TABLE II
PHYSICAL CHARACTERISTICS OF THE SUBJECT

Sex	Age	Height	Weight
Male	23	183cm	77kg

IV. APPLICATION AND PRELIMINARY RESULTS

In this section, to investigate the potential of the optical waveguide sensor with a carbon fiber layer for human-computer interaction or rehabilitation applications, we attached the sensors to a human upper limb to detect the change in grip strength when clenching the fist. Two placement locations were considered, one close to the wrist and one close to the elbow. We recruited one healthy volunteer to conduct preliminary experiments. The experiments were approved by the Local Ethics Committee of Beihang University. The subject read and signed informed consent forms before the experiments. The physiological characteristics of the subject are shown in Table II.

A. Sensor Position

1) Close to the Elbow: Clinical conditions often exist that require assessment of finger muscle strength and atrophy. The current assessment approach focuses on assessing the

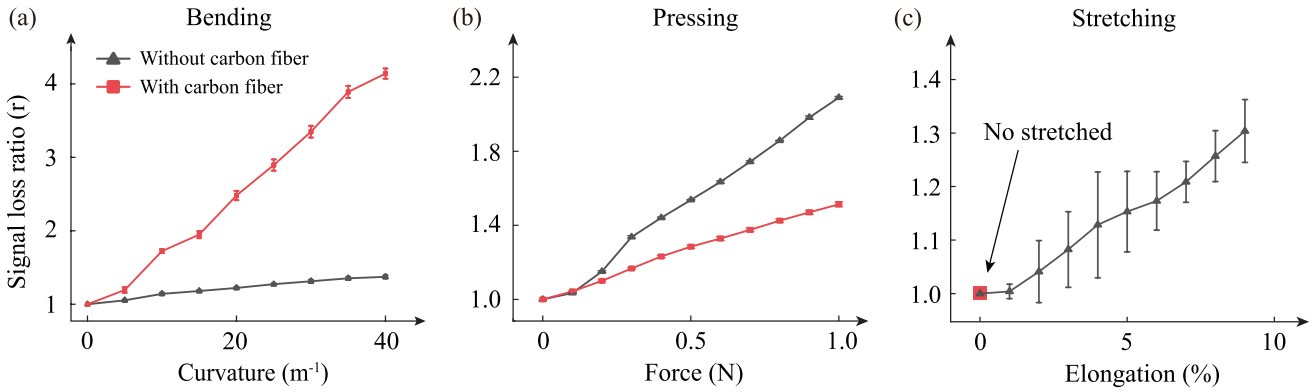

Fig. 5. Characterization of the optical waveguide sensor in different deformation modes. Characterization for (a) bending, (b) pressing, and (c) stretching. (Error bars indicate SDs from 10 cyclic tests of one waveguide sample).

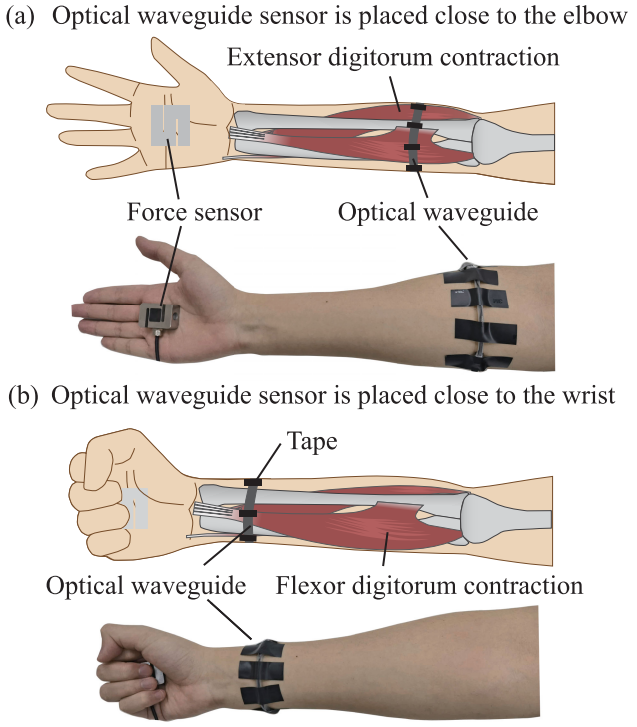

Fig. 6. Position of the optical waveguide sensor and force sensor, and muscle movement when clenching fist. (a) The optical waveguide sensor is placed close to the elbow, and the extensor digitorum is contracted when opening a hand. (b) The optical waveguide sensor is placed close to the wrist, and the Flexor digitorum is contracted when clenching a fist.

thickness and activity of the flexor digitorum muscle, which includes both the superficialis and profundus components. It is also necessary to examine the strength of the extensor digitorum muscle as a second assessment standard [28]. This illustrates that the main muscles that generate force when a person clenches a fist are flexor digitorum muscle and extensor digitorum muscle. The positions of these two muscles are shown in Fig. 6, which are close to the elbow. So, we attached the ends of the optical waveguide sensor to flexor digitorum muscle and extensor digitorum muscle, so that the deformation caused by the muscle contraction (mostly flexion, a small part is pressure, and stretching is constrained by the carbon fiber layer) when we clench our fists, could be monitored by the sensor to the maximum extent. In addition, an S-shaped force sensor (AT8314, Autoda Ltd.) is held in hand to measure the grip strength compared to the sensor signal. This force sensor has a range of 200N and an output sensitivity of $2.0 \pm 10\%$ mV/V, which ensures accurate measurements.

2) Close to the Wrist: Forces generated in muscles are transmitted to bone through tendons, which makes joint and limb movement possible. To do this effectively, tendons must bear large forces. In human hand flexor tendons, it was shown that the intratendinous force of the tendon depends on whether the force was generated passively or actively, and on whether the position of the joint was in flexion or extension. During passive mobilization of the wrist, the flexor tendon force was found to range between 1 and 6N, and up to 9N during similar mobilization of the fingers. During a 35N tip-pinch, the tendon force measured up to 12N, whereas during active, unresisted finger motion, the tendon force reached about 35N [29]. The force of the tendon is so great and so much closer to the fist that holds the force sensor that a new idea was discovered as to whether the magnitude of the grip force could be reflected by monitoring changes in the tendon that connects the fingers. So, we attached the optical waveguide sensor close to the wrist, a position that wraps around the tendon. When the fist is clenched and opened, the muscle contracts and expands, driving the tendon and transmitting force. In this process, the changes in the tendon are transmitted to the skin and then to the optical waveguide sensor, and the sensor signal reflects the changes, thus mapping the changes in grip force.

The following three points can ensure the comfort of the subject wearing the sensor for a long time: (1) The weight of the sensor attached to the arm is only 6.8g. And this weight does not put any burden on the subject. (2) The optical waveguide sensor communicates with the computer via Bluetooth, which removes the signal line between the person and the computer and allows the subject to move more freely. (3) The cladding of the optical waveguide sensor in contact with the skin is very soft, which does not cause too much pressure on the skin.

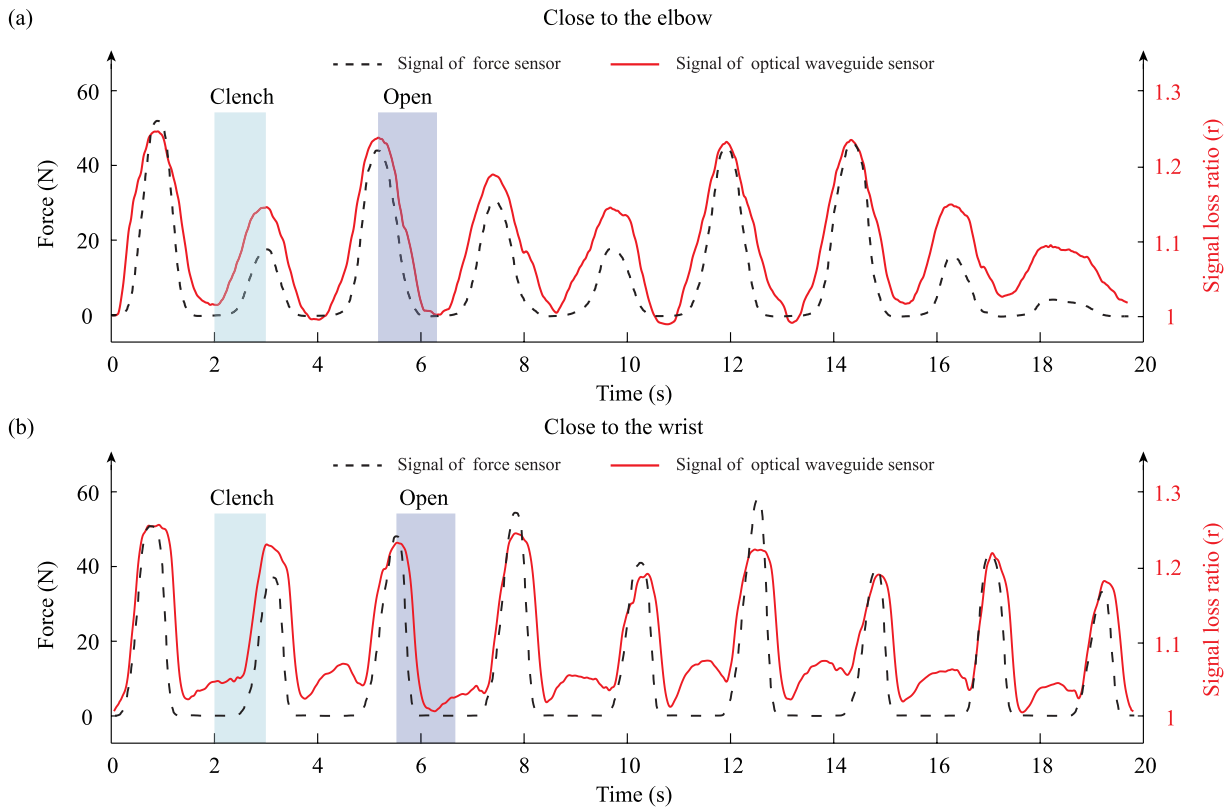

Fig. 7. Subsets of cyclic test results for monitoring grip strength. (a) Optical waveguide sensor signal and force sensor signal when the optical waveguide sensor is placed close to the elbow. (b) Optical waveguide sensor signal and force sensor signal when the optical waveguide sensor is placed close to the wrist.

B. Raw Signal

After fixing the optical waveguide sensor and the force sensor, we performed a fist-clenching and hand-opening test, with 10 cycles as a set and 20 repetitions. We conducted a set of experiments with the optical waveguide sensor placed close to the elbow and a set of comparison experiments with the optical waveguide sensor placed close to the wrist to investigate the difference in signal when the sensor is placed in these two positions. Fig. 7 shows subsets of cycle test results.

1) Close to the Elbow: Fig. 7a shows the raw signal variation curves of the force sensor and the optical waveguide sensor when the optical waveguide sensor is placed close to the elbow position in the fist-clenching and hand-opening test. It can be seen that in each cycle, the signal of the optical waveguide sensor has a clear correspondence with the signal of the force sensor. The peaks of the two curves indicate the maximum muscle deformation and the maximum grip strength respectively, both of which also correspond to each other. Several noises can be observed in the signal curves of the optical waveguide sensor, which come from the shaking of the muscle contraction and the movement of the upper limb. This phenomenon also demonstrates the sensitivity of the optical waveguide sensor, which can monitor changes that cannot be detected by ordinary sensors. In addition, the optical waveguide sensor also exhibits a certain hysteresis type: after the hand was fully opened, the signal of the force sensing had gone to zero, but the signal of the optical waveguide sensor did not go to zero immediately, but gradually decreased to zero. There are two reasons for this phenomenon. The first reason is the characteristics of the optical waveguide material, and the elastomer does not immediately return to its initial state after deformation. There is still a loss of light. The second reason is that the fingers do not keep touching the force sensor during the process of opening the hand. When the fingers are separated from the force sensor, the fingers are still being opened and the muscle contraction continues, and this process is being monitored by the optical waveguide sensor. However, the force sensor does not monitor it. Also, there was hysteresis in the process of making a fist, but the reason for this phenomenon is mainly the time difference between the fingers touching the force sensor when the open hand starts to make a fist. The hysteresis in the deformation of the elastomer does not affect the fist clenching process.

2) Close to the Wrist: Fig. 7b shows the raw signal variation curves of the force sensor and the optical waveguide sensor when the optical waveguide sensor is placed close to the wrist position in the fist-clenching and hand-opening test. It can be seen that in each cycle, the signal of the optical waveguide sensor has the same trend as the signal of the force sensor, but the peak value at each fist clench does not correspond well. The sensitivity and hysteresis of the optical waveguide sensor still exist. When the optical waveguide sensor is placed close to the elbow, the optical waveguide sensor signal lags behind the force sensor signal by a total of 2.1 s for the nine fist clenching experiments shown in Fig. 7a. In contrast, the optical waveguide sensor signal lags behind the force sensor

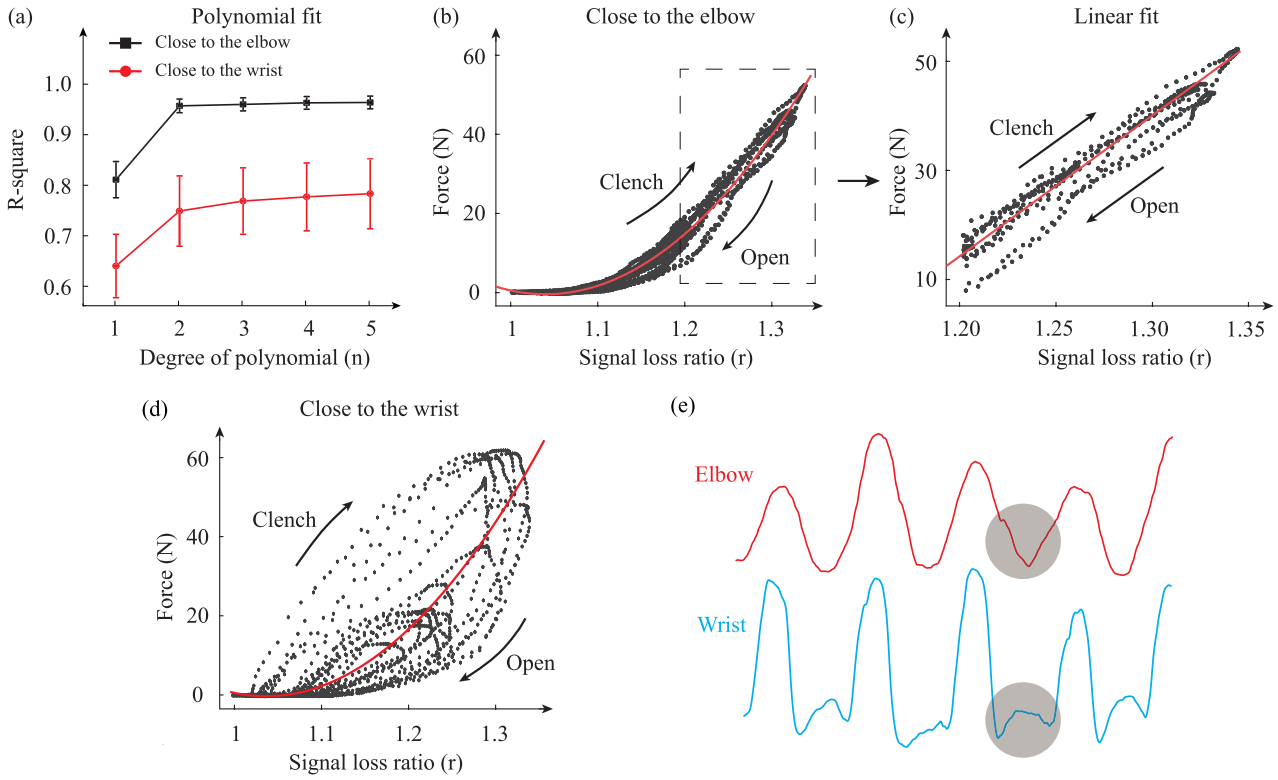

Fig. 8. Results of the polynomial fitting. (a) R-squared for fitting polynomials of different degrees. (b) When the optical waveguide sensor is placed close to the elbow, the grip force signal is fitted to the sensor signal using a quadratic polynomial, and R-squared is 0.9827. (c) Linear fit to partial data from (b) (light intensity loss ratio from 1.20 to 1.35), R-squared is 0.9523. (d) When the optical waveguide sensor is placed close to the wrist, the grip force signal is fitted to the sensor signal using a quadratic polynomial, and R-squared is 0.7721. (e) Optical waveguide sensor signal of the fist clenching experiment when the optical waveguide sensor is placed close to the elbow and close to the wrist, respectively. (Error bars indicate SDs from 20 cyclic tests of one waveguide sample).

signal by a total of 1 s for the original signal shown in Fig. 7b when the optical waveguide sensor is placed close to the wrist. The difference in lag time between the two experiments reached 100%, which was mainly due to the fact that the deformation caused by the tendon was more minimal compared to that caused by flexor digitorum muscle and extensor digitorum muscle. The small deformation allows the elastomer to return to its initial state more quickly. So, the signal hysteresis of the optical waveguide sensor is not significant. It is important to note that in Fig. 7b, it is evident that the signal from the force sensor drops to 0 when the fist is opened, while the signal from the optical waveguide sensor does not drop to 0, but instead appears to rise. This change is not desired, which can affect the judgment of the optical waveguide sensor on the grip force at low grip force. On the contrary, in Fig. 7a, the signal of the optical waveguide sensor drops to 0, which does not affect the judgment of the grip force. The difference between the variations of these two waveforms is specifically marked in Fig. 8e.

From the raw signals of the comparison test that placed the light waveguide sensor with the two positions, it is evident that the change in the signal obtained when the optical waveguide sensor is placed close to the elbow is more reflective of the change in grip force. The tendon is closer to the fist but does not better reflect the grip force. The results of the raw signals directly indicate that flexor digitorum muscle and extensor digitorum muscle bring significantly more variation to the optical waveguide sensor than the tendon.

C. Polynomial Fitting

To further investigate the relationship between the optical waveguide sensor signal and grip strength, we made a polynomial fitting to 20 sets of data, and the results are shown in Fig. 8.

1) Close to the Elbow: Fig. 8a shows the R-squared of the fitting using polynomials of different degrees from 1 to 5 when the optical waveguide sensor is placed close to the elbow. As can be seen from the figure, the R-squared using the linear fitting was about 0.8, which is not an ideal value, so we increased the degree of polynomials and obtained an R-squared greater than 0.95. Obviously, when the degree of polynomials was 2, the R-squared was vastly improved compared to the degree of 1. However, this improvement did not occur at higher degrees. Therefore, only a quadratic polynomial fitting is needed to initially build the relationship between the optical waveguide sensor signal and the grip strength. Fig. 8b shows the results of the fitting using a quadratic polynomial. We plotted all data points from a set of tests in a single graph, and the signal did not drift significantly over 10 cycles, demonstrating good repeatability. The fitted polynomial was

$$F(x) = 594.2x^2 - 1236x + 642.2 \tag{5}$$

And the R-squared was 0.9827. The fact that an R-squared greater than 0.95 can be obtained using a quadratic polynomial fitting is already a good result, which indicates that it is not difficult to build an accurate connection between the optical waveguide sensor signal and the grip strength. Besides, we can find that the curve in the 1.2 to 1.35 part of the light intensity loss ratio in Fig. 8b is essentially linear. So we fitted the data of this section separately for linearity, and the result is shown in Fig. 8c. The fitted polynomial was

$$F(x) = 258.5x - 295.9 \tag{6}$$

And the R-squared was 0.9523. The R-squared of greater than 0.95 fully illustrates the linearity of the data when the light intensity is between 1.2 and 1.3, which indicates that the optical waveguide sensor is easily calibrated.

2) Close to the Wrist: As shown in Fig. 8a, even with a polynomial degree of 5, the R-squared cannot exceed 0.8 when the optical waveguide sensor is placed close to the wrist. This fit does not guarantee that the signal from the optical waveguide sensor can map the grip force with a very small error. Fig. 8d shows fit results using a quadratic polynomial with an R-squared of 0.7721. Compared to the fit with the optical waveguide sensor placed close to the elbow, the data points are significantly more spread out, and no interval can be found in the plot that shows a linear relationship. Fig. 8e shows the comparison of the optical waveguide sensor signal waveforms when the optical waveguide sensor is placed close to the elbow or wrist. Instead of a smooth drop, the optical waveguide sensor rises at the trough when placed close to the wrist, forming a small wave peak. The movement of the tendon causes the rise of the trough. When opening the fist, the flexor digitorum relax and the tendons in the wrist move towards the palm, driving some of the flexor digitorum towards the wrist, which leads to a slight increase in the curvature of the wrist, resulting in a small rise in the optical waveguide sensor signal. It is not a coincidence that this small crest persisted in every grip experiment, which severely reduces the R-squared of the polynomial fit. The small R-squared indicates that it is almost impossible to monitor the grip force by trying to place the optical waveguide sensor close to the wrist.

By comparing the polynomial fits of the experimental results for the two placements of the optical waveguide sensor, it is further demonstrated that it is feasible to monitor grip force by monitoring the deformation brought about by flexor digitorum muscle and extensor digitorum muscle by placing the optical waveguide sensor close to the elbow. On the contrary, the sensor signal variation brought by the tendon located close to the wrist does not reflect the grip force variation stably. Therefore, if the optical waveguide sensor is placed close to the elbow, the high R-squared indicates that it is feasible to predict the grip force through the optical waveguide sensor signal, which could provide a new method of interaction between the user and the prosthesis with the advantages of anti-electromagnetic interference, antiperspirant, inherent electrical safety, and the potential for biocompatibility.

V. Discussion

In this paper, we extend the previous studies [18], [21], [22]. Previous studies only focused on total internal reflection and how to apply this phenomenon, neglecting the intrinsic connection between several factors that cause changes in light intensity (bending, stretching and pressure). However, in general, these three deformations are not expected to appear simultaneously, which makes it more difficult to build a relationship between light intensity and a particular deformation. So, if some of these factors are constrained, does the sensitivity of the optical waveguide to the remaining factors increase? To find the answer, we embedded an almost unstretchable carbon fiber layer into the optical waveguide, which fully constrains the stretching deformation and partly constrains pressing deformation.

A. Sensor Characteristics

Compared with the optical waveguide sensor without a carbon fiber layer, the sensor in this study showed better sensitivity and linearity during bending and pressure due to the anti-stretch carbon fiber layer of the optical waveguide reducing the influence factor of light intensity loss. There are two possible reasons for this phenomenon:

(1) Compared to polyurethane elastomers, carbon fiber has a more irregular surface. We can approximate the surface of polyurethane elastomer as glossy, while the surface of carbon fiber is irregular. As shown in Fig. 9a, specular reflection occurs when light is incident on a glossy surface, and diffuse reflection occurs when light is incident on an irregular surface. Obviously, the diffuse reflection leads to a great loss of light intensity. Further, when light is transmitted in an optical waveguide without carbon fiber, it can be considered that specular reflection occurs, and when light is transmitted in an optical waveguide with carbon fiber, it can be considered that diffuse reflection occurs. Therefore, as shown in Fig. 9b, when light is transmitted in an optical waveguide with carbon fiber, the more reflections occur, the more light loss occurs due to diffuse reflection, but this loss does not occur in an optical waveguide without the carbon fiber. And the greater the curvature of the optical waveguide, the more reflections of light occur in the optical waveguide, which leads to a higher sensitivity to curvature in the optical waveguide with carbon fiber.

(2) Compared to other colors, black carbon fiber is more likely to absorb light rather than reflect it. Therefore, when there is light incident into the carbon fiber, most of the light intensity is absorbed. A part of the light intensity is absorbed when light is shot into the carbon fiber. As a result, as the curvature of the optical waveguide increases, the reflections of light increase, and the light intensity lost increases.

In tests to monitor grip strength, the optical waveguide sensor signal showed a high correlation with grip strength and was able to detect small muscle deformations when the optical waveguide sensor was placed close to the elbow. These results demonstrated the feasibility of applying the sensor to monitor muscle deformation and strength. So in prosthetic research, where the need to discriminate subtle forces often

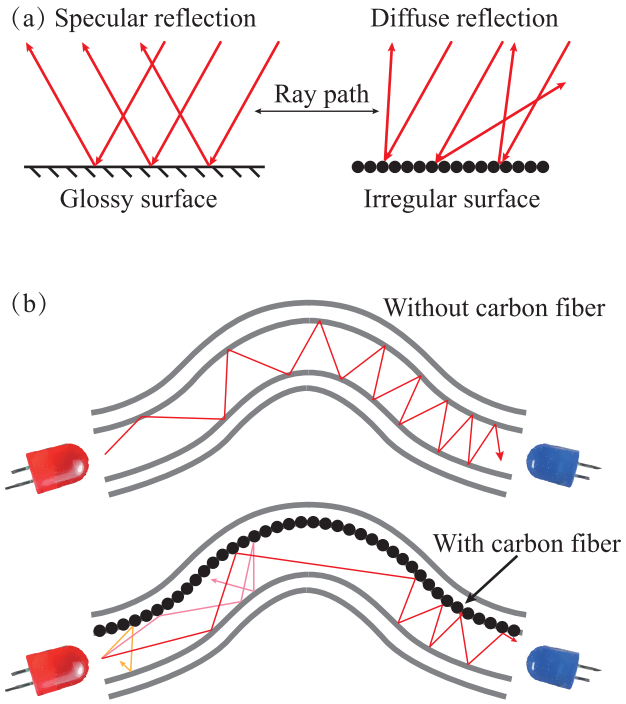

Fig. 9. Reflection path of light. (a) Specular reflection and diffuse reflection. (b) Comparison of ray paths in optical waveguides with and without carbon fiber.

arises, this sensor has the ability to enable the prosthesis to interact with the user. By virtue of its sensitivity to muscle deformation, a prosthesis with this integrated sensor can monitor the deformation of the user's muscles to determine the force that the user wishes to exert. This allows the prosthesis to easily pick up objects of different masses without causing damage. And research on prosthetics will be conducted in the future. In addition, the simple manufacturing process and the possibility of selecting various shapes of molds make it possible to manufacture optical waveguides of various shapes. Various shapes of optical waveguides mean that they can be attached to various parts of the body, and a larger monitoring area can be obtained by increasing the surface area of the optical waveguide.

B. Influence of Manufacturing Inaccuracies

In the tests, we summarized some factors that affect the accuracy and repeatability of the sensor:

(1) Error at the time of making elastomer. The two raw materials are mixed in a certain ratio and stirred well when making elastomer. Inevitably, errors in the measurement of the two materials lead to deviations in the refractive index of the elastomer from the desired value. This characterization is also affected by whether the mixture is homogeneous. In addition, the air bubbles created during the casting process cannot be completely evacuated, which causes unnecessary light loss in the optical waveguide.

(2) Irregular cross-section of the core. During the casting process, the surface of the core in contact with air does not form a standard flat surface due to surface tension but an arc with a slight curvature. Although it does not affect the sensitivity and repeatability of the optical waveguide, it can cause unnecessary light loss.

(3) Unstable connection of LEDs and photodiodes to the optical waveguide. The optical waveguide sensor uses glue to connect to the 3d printing sleeve, and the concentricity when manually aligning the diode, sleeve, and optical waveguide cannot be guaranteed, which can cause unnecessary loss of light intensity.

All these points can cause signal deviations and undesired characteristics between undeformed different sensors. This suggests that each sensor should be calibrated separately when applying the sensor to reality. The high repeatability obtained in the tests makes it unnecessary to worry about these issues since the sensor can be used directly as soon as its response characteristics are determined. Moreover, the high correlation between the sensor signal and the force signal in the tests to monitor grip force makes calibration very easy. In the future, we will try to improve the molds and increase the accuracy of the manufacturing process as a way to reduce the errors brought by the fabrication of the sensor.

VI. Conclusion

In this study, an optical waveguide sensor with a carbon fiber layer was developed to provide a new idea for optical waveguide sensor research. By embedding the carbon fiber layer to constrain the stretching of the optical waveguide fully, pressing deformation partly, and allowing bending deformation. From the test results, it can be concluded that the sensitivity of the proposed sensor to bending is three times higher than that of the typical optical waveguide sensor due to the complete elimination of the stretching factor, and the pressure deformation is partially limited to make the proposed sensor more linear in response to pressure. And the simple manufacturing process and good repeatability are retained while improving performance. The optical waveguide sensor has a lifetime of more than one year and is reusable. Furthermore, it can respond well to grip force when attached to the upper limb. A polynomial fitting was used to initially determine the relationship between the sensor signal and grip force. And the best result was coefficient of determination $R^2 = 0.9827$(quadratic polynomial fitting), and when the grip force is greater than 10 N, a linear relationship can be obtained (the R-squared of the linear fitting was 0.9523). These results have great implications for the accurate prediction of grip strength using the proposed sensor. A potential application for the proposed sensor is the ability to recognize the human intention to control prostheses for amputees.

References

[1] C. L. McDonald, S. Westcott-McCoy, M. R. Weaver, J. Haagsma, and D. Kartin, "Global prevalence of traumatic non-fatal limb amputation," *Prosthetics Orthotics Int.*, vol. 2021, Apr. 2021, Art. no. 0309364620972258.

[2] A. J. Thurston, "Paré and prosthetics: The early history of artificial limbs," *ANZ J. Surg.*, vol. 77, no. 12, pp. 1114–1119, Dec. 2007.

[3] P. Polygerinos et al., "Soft robotics: Review of fluid-driven intrinsically soft devices; manufacturing, sensing, control, and applications in human–robot interaction," *Adv. Eng. Mater.*, vol. 19, no. 12, 2017, Art. no. 1700016.

[4] M. Vidal, J. Turner, A. Bulling, and H. Gellersen, "Wearable eye tracking for mental health monitoring," *Comput. Commun.*, vol. 35, no. 11, pp. 1306–1311, 2012.

[5] D. Chen and Q. Pei, "Electronic muscles and skins: A review of soft sensors and actuators," *Chem. Rev.*, vol. 117, no. 17, pp. 11239–11268, 2017.

[6] M. Haghi, K. Thurow, and R. Stoll, "Wearable devices in medical Internet of Things: Scientific research and commercially available devices," *Healthcare Inf. Res.*, vol. 23, no. 1, pp. 4–15, 2017.

[7] Y. Wang, H. Wu, L. Xu, H. Zhang, Y. Yang, and Z. L. Wang, "Hierarchically patterned self-powered sensors for multifunctional tactile sensing," *Sci. Adv.*, vol. 6, no. 34, Aug. 2020, Art. no. eabb9083.

[8] L. Shi, Z. Li, M. Chen, Y. Qin, Y. Jiang, and L. Wu, "Quantum effect-based flexible and transparent pressure sensors with ultrahigh sensitivity and sensing density," *Nature Commun.*, vol. 11, no. 1, pp. 1–9, Jul. 2020.

[9] A. Atalay et al., "Batch fabrication of customizable silicone-textile composite capacitive strain sensors for human motion tracking," *Adv. Mater. Technol.*, vol. 2, no. 9, Sep. 2017, Art. no. 1700136.

[10] C. B. Cooper et al., "Stretchable capacitive sensors of torsion, strain, and touch using double helix liquid metal fibers," *Adv. Funct. Mater.*, vol. 27, no. 20, 2017, Art. no. 1605630.

[11] C. M. Boutry et al., "A hierarchically patterned, bioinspired e-skin able to detect the direction of applied pressure for robotics," *Sci. Robot.*, vol. 3, no. 24, Nov. 2018, Art. no. eaau6914.

[12] Z. Zhao, Z. Yu, K. Chen, and Q. Yu, "A fiber-optic Fabry–Pérot accelerometer based on high-speed white light interferometry demodulation," *J. Lightw. Technol.*, vol. 36, no. 9, pp. 1562–1567, May 1, 2018.

[13] Q. Liu, X. Qiao, Z. Jia, H. Fu, H. Gao, and D. Yu, "Large frequency range and high sensitivity fiber Bragg grating accelerometer based on double diaphragms," *IEEE Sensors J.*, vol. 14, no. 5, pp. 1499–1504, May 2014.

[14] H. Wu, Y. Guo, L. Xiong, W. Liu, G. Li, and X. Zhou, "Optical fiber-based sensing, measuring, and implementation methods for slope deformation monitoring: A review," *IEEE Sensors J.*, vol. 19, no. 8, pp. 2786–2800, Apr. 2019.

[15] A. L. Washburn and R. C. Bailey, "Photonics-on-a-chip: Recent advances in integrated waveguides as enabling detection elements for real-world, lab-on-a-chip biosensing applications," *Analyst*, vol. 136, no. 2, pp. 227–236, 2011.

[16] C. K. Leung et al., "Optical fiber sensors for civil engineering applications," *Mater. Struct.*, vol. 48, no. 4, pp. 871–906, 2015.

[17] M. F. Bado and J. R. Casas, "A review of recent distributed optical fiber sensors applications for civil engineering structural health monitoring," *Sensors*, vol. 21, no. 5, p. 1818, 2021.

[18] H. Krauss and K. Takemura, "Stretchable optical waveguide sensor capable of two-degree-of-freedom strain sensing mediated by a semidivided optical core," *IEEE/ASME Trans. Mechatronics*, vol. 27, no. 4, pp. 2151–2157, Aug. 2022.

[19] S. K. Selvaraja and P. Sethi, "Review on optical waveguides," in *Emerging Waveguide Technology*. Rijeka, Croatia: InTech, Aug. 2018.

[20] T. Kim, S. Lee, T. Hong, G. Shin, T. Kim, and Y.-L. Park, "Heterogeneous sensing in a multifunctional soft sensor for human–robot interfaces," *Sci. Robot.*, vol. 5, no. 49, Dec. 2020, Art. no. eabc6878.

[21] H. Zhao, K. O'Brien, S. Li, and R. F. Shepherd, "Optoelectronically innervated soft prosthetic hand via stretchable optical waveguides," *Sci. Robot.*, vol. 1, no. 1, Dec. 2016, Art. no. eaai7529.

[22] H. Bai, S. Li, J. Barreiros, Y. Tu, C. R. Pollock, and R. F. Shepherd, "Stretchable distributed fiber-optic sensors," *Science*, vol. 370, no. 6518, pp. 848–852, Nov. 2020.

[23] D. Chung, *Carbon Fiber Composites*. Amsterdam, The Netherlands: Elsevier, 2012.

[24] M. A. Habib, M. S. Anower, and M. R. Hasan, "Highly birefringent and low effective material loss microstructure fiber for THz wave guidance," *Opt. Commun.*, vol. 423, pp. 140–144, Sep. 2018.

[25] C. To, T. L. Hellebrekers, and Y.-L. Park, "Highly stretchable optical sensors for pressure, strain, and curvature measurement," in *Proc. IEEE/RSJ Int. Conf. Intell. Robots Syst. (IROS)*, Sep. 2015, pp. 5898–5903.

[26] A. D. Marchese, R. K. Katzschmann, and R. Daniela, "A recipe for soft fluidic elastomer robots," *Soft Robot.*, vol. 2, no. 1, pp. 7–25, 2015.

[27] D. Rus and M. T. Tolley, "Design, fabrication and control of soft robots," *Nature*, vol. 521, pp. 467–475, May 2015.

[28] C. I. Ioannou, F. L. Hodde-Chriske, M. N. Avraamides, and E. Altenmüller, "Novel ultrasonographic thickness and strength assessments of the flexor digitorum: A reliability analysis," *Med. Problems Performing Artists*, vol. 36, no. 4, pp. 269–278, Dec. 2021.

[29] J. H.-C. Wang, "Mechanobiology of tendon," *J. Biomechanics*, vol. 39, no. 9, pp. 1563–1582, 2006.